Shape and SPR Evolution of Thorny Gold Nanoparticles Promoted by Silver Ions

Hong Yuan,[†] Wanhong Ma,[†] Chuncheng Chen,[†] Jincai Zhao,*[,†] Jiangwen Liu,[‡] Huaiyong Zhu,[‡] and Xueping Gao[§]

Beijing National Laboratory for Molecular Sciences, Key Laboratory of Photochemistry, Institute of Chemistry, The Chinese Academy of Sciences, Beijing 100080, P. R. China, School of Physical and Chemical Sciences, Queensland University of Technology, Brisbane QLD 4001, Australia, and Institute of New Energy Material Chemistry, Department of Material Chemistry, Nankai University, Tianjin 300071, China

Received August 29, 2006. Revised Manuscript Received January 12, 2007

The gold-seed-mediated growth approach is developed to obtain three-dimensional (3D) thorny gold nanoparticles, and their morphology can be tailored by introducing different amounts of Ag^+ ions into the reaction systems of $HAuCl_4$ and NH_2OH in the absence of templates and surfactants. Changing the concentration of silver ions from 0 to 2.5×10^{-6} M leads to the gradual deviations of the resulted nanoparticle morphology from the spherical geometry. The morphology of gold nanoparticles can be tuned from sphere to the anomalous nonspheres, to the gold nanoparticles with short thorns, to the gold nanoparticles with long thorns of more than 100 nm. At too high concentrations (above 2.5×10^{-6} M), the number of the nanothorns on each gold nanoparticle decreased and the central parts of the 3D gold nanostructures (the body) expanded. For the gold nanoparticles with short thorns, most of the short thorns are single crystals and the rest are 2- or 5-fold twinned crystals. However, the long gold thorns consist mainly of 2-fold twinned crystals and a few 5-fold twinned crystals. The 3D thorny gold nanoparticles exhibit a broad absorption peak at 600−1100 nm in the visible and near-infrared range, and their spectral properties can be tuned by altering their shapes. These 3D thorny gold nanoparticles have great potential for the applications in chemical imaging and biomedical sciences.

Introduction

Nanomaterials have stimulated great interest in many areas such as catalysis, biological, and chemical sensing, and nanotechnology.[1−5] Noble metallic nanoparticles exhibit unique and distinctive spectral properties and the potential application of these properties have been extensively studied.[6] The theories and experimental data have validated that surface plasmon resonances (SPR) spectra of the particles can be readily tuned from the near-UV to the visible spectrum, and even into the mid-infrared (mid-IR) region by altering their size, shape, spacing, and dielectric environments.[6−9] Actually, the particle morphology of gold nanostructures has more significant influence on the properties of the SPR band than their sizes.[9] The deviations from spherical geometry (in particular, the appearance of sharp apexes) generally lead to considerable red-shift of the SPR peaks in the visible−near-IR region.[7−10] Another important application of noble metal nanostructures is surface-enhanced Raman spectroscopy (SERS),[11] which has been a powerful

* Correponding author. E-mail: jczhao@iccas.ac.cn.
[†] The Chinese Academy of Sciences.
[‡] Queensland University of Technology.
[§] Nankai University.

(1) Reviews: (a) El-Sayed, M. A. *Acc. Chem. Res.* **2001**, *34*, 257. (b) Burda, C.; Chen, X. B.; Narayanan, R.; El-Sayed, M. A. *Chem. Rev.* **2005**, *105*, 1025. (c) Xia, Y. N.; Halas, N. J. *MRS Bull.* **2005**, *30*, 338. (d) Rosi, N. L.; Mirkin, C. A.; *Chem. Rev.* **2005**, *105*, 1547. (e) Katz, E.; Willner, I. *Angew. Chem., Int. Ed.* **2004**, *43*, 6042. (f) Daniel, M. C.; Astruc, D. *Chem. Rev.* **2004**, *104*, 293.

(2) Catalysis: (a) Yoon, B.; Hakkinen, H.; Landman, U.; Worz, A. S.; Antonietti, J. M.; Abbet, S.; Judai, K.; Heiz, U. *Science* **2005**, *307*, 403. (b) Hughes, M. D.; Xu, Y. J.; Jenkins, P.; McMorn, P.; Landon, P.; Enache, D. I.; Carley, A. F.; Attard, G. A.; Hutchings, G. J.; King, F.; Stitt, E. H.; Johnston, P.; Griffin, K.; Kiely, C. J. *Nature* **2005**, *437*, 1132. (c) Campbell, C. T. *Science* **2004**, *306*, 234. (d) Chen, M. S.; Goodman, D. W. *Science* **2004**, *306*, 252. (e) Daté, M.; Okumura, M.; Tsubota, S.; Haruta, M. *Angew. Chem., Int. Ed.* **2004**, *43*, 2129.

(3) Chemical sensing: (a) Lin, S. Y.; Liu, S. W.; Lin, C. M.; Chen, C. H. *Anal. Chem.* **2002**, *74*, 330. (b) Kim, Y.; Johnson, R. C.; Hupp, J. T. *Nano Lett.* **2001**, *1*, 165. (c) Obare, S. O.; Hollowell, R. E.; Murphy, C. J.; *Langmuir* **2002**, *18*, 10407. (d) Majid, E.; Hrapovic, S.; Liu, Y. L.; Male, K. B.; Luong, J. H. T. *Anal. Chem.* **2006**, *78*, 762.

(4) Biological sensing and medicine: (a) Thaxton, C. S.; Rosi, N. L.; Mirkin, C. A. *MRS Bull.* **2005**, *30*, 376. (b) Keating, C. D. *Proc. Natl. Acad. Sci. U.S.A.* **2005**, *102*, 2263. (c) Liu, J. W.; Lu, Y. *Angew. Chem., Int. Ed.* **2006**, *45*, 90. (d) Hirsch, L. R.; Stafford, R. J.; Bankson, J. A.; Sershen, S. R.; Rivera, B.; Price, R. E.; Hazle, J. D.; Halas, N. J.; West, J. L. *Proc. Natl. Acad. Sci. U.S.A.* **2003**, *100*, 13549. (e) Loo, C.; Lowery, A.; Halas, N.; West, J.; Drezek, R. *Nano Lett.* **2005**, *5*, 709.

(5) Nanotechnology: (a) Barnes, W. L.; Dereux, A.; Ebbesen, T. W. *Nature* **2003**, *424*, 824. (b) Link, S.; Burda, C.; Nikoobakht, B.; El-Sayed, M. A. *Chem. Phys. Lett.* **1999**, *315*, 12. (c) Ditlbacher, H.; Krenn, J. R.; Lamprecht, B.; Leitner, A.; Aussenegg, F. R. *Opt. Lett.* **2000**, *25*, 563. (d) Chen, S. W.; Ingram, R. S.; Hostetler, M. J.; Pietron, J. J.; Murray, R. W.; Schaaff, T. G.; Khoury, J. T.; Alvarez, M. M.; Whetten, R. L. *Science* **1998**, *280*, 2098.

(6) (a) Schmid, G. *Nanoparticles: From Theory to Application*; Wiley-VCH Verlag GmbH & Co. KGaA: Weinheim, Germany, 2004. (b) Feldheim, D. L.; Foss, C. A., Jr. *Metal Nanoparticles: Synthesis, Characterization, and Applications*; Marcel Dekker: New York, 2002.

(7) Kelly, K. L.; Coronado, E.; Zhao, L. L.; Schatz, G. C. *J. Phys. Chem. B* **2003**, *107*, 668.

(8) Link, S.; El-Sayed, M. A. *Annu. Rev. Phys. Chem.* **2003**, *54*, 331.

(9) Liz-Marzán, L. M. *Langmuir* **2006**, *17*, 32.

(10) (a) Jin, R.; Cao, Y.; Mirkin, C. A.; Kelly, K. L.; Schatz, G. C.; Zheng, J. G. *Science* **2001**, *294*, 1901. (b) Jin, R.; Cao, Y. C.; Hao, E.; Metraux, G. S.; Schatz, G. C.; Mirkin, C. A. *Nature* **2003**, *425*, 487.

10.1021/cm062046i CCC: $37.00
Published on Web 03/03/2007

tool in the research of surface sciences[12] and analytical chemistry.[13] Some nanostructures, with sharp apexes,[14] fractal spaces at nanoparticle junctions,[15] and tips of nanorods,[16] are especially active SERS substrates.

The properties and applications of nanomaterials depend profoundly on their morphologies;[1−16] thus, the control of their sizes and shapes is essentially required, and many methods have been developed to synthesize gold nanoparticles of various morphologies, which include zero (0D) dimensional,[17] 1D,[18−30] 2D,[31−39] and 3D structures.[14,40−47] Nonetheless, there are substantial difficulties in forming gold nanostructures of complicated morphologies in isotropic aqueous solution because of the intrinsic properties of noble metal crystals, which usually possess a highly symmetric face-centered cubic (fcc) structure. To the best of our knowledge, almost all synthesis methods for control of gold nanoparticle morphology require using templates or surfactants.[18−47] For example, shaped gold nanocrystals were synthesized in the presence of organic surfactants as shape-directing reagents such as cetyltrimethylammonium bromide (CTAB),[19−22,24−28,48,52] bis-(*p*-sulfonatophenyl) phenylphosphine dihydrate dipotassium (BSPP),[49] poly(*N*-vinyl-2-pyrrolidone) (PVP),[50] and sodium dodecyl sulfate (SDS).[51] In these reported methods, CTAB is one of the most widely applied surfactants[19−22,24−28,47,48,52] because of its preferential binding based on sterics; the Au atom spacing on the side faces is more comparable to the size of the CTA^+ headgroup than the close-packed [111] face of gold.[27] An alternative approach is using templates to direct the formation of gold nanocrystals with anisotropic morphologies.[14,18,40−46] However, their application is restricted because of a number of limiting factors including the tedious work involved in the preparation, removal of the templates, or the limited range of morphological variation, especially in preparing metal nanocrystals with higher-order complexities such as branched structures.

It is no doubt that the presence of templates or surfactants is one of crucial factors in obtaining the shaped gold nanoparticles,[17−47] but other experimental parameters, to a certain extent, affect their growth process. For example, it was found that in the presence of CTAB, the addition of Ag^+ ions not only increases the yield of gold nanorods[27] but also changes their aspect ratio.[21,28] These studies highlight that the presence of Ag^+ ions greatly affects the growth of gold nanoparticles.[27] However, according to Mulvaney and his co-workers,[24] the role of the silver ions may not be significant. They found that $AgNO_3$ is not needed to control the aspect ratio of gold nanorods and that their size and aspect ratio could be controlled through using different sized seed particles in the presence of CTAB.[24]

In the present study, we propose a simple synthesis process for shaped gold nanocolloids promoted by silver ions in the absence of surfactants and templates based on the self-catalyzed growth of gold nanoseeds in the reaction system of $HAuCl_4$ and NH_2OH. Various amounts of silver ions, which can control the morphology of resulted 3D thorny gold nanoparticles and the structure of the gold nanothorns on their surfaces, were introduced into the reaction systems to tailor the growth of gold seed nanoparticles. The gold nanoparticles obtained were characterized by a variety of

(11) Schatz, G. C. *Acc. Chem. Res.* **1984**, *17*, 370.
(12) (a) Kneipp, K.; Kneipp, H.; Itzkan, I.; Dasari, R. R.; Feld, M. S. *Chem. Rev.* **1999**, *99*, 2957. (b) Baia, M.; Baia, L.; Kiefer, W.; Popp, J. *J. Phys. Chem. B* **2004**, *108*, 17491.
(13) Vankeirsbilck, T.; Vercauteren, A.; Baeyens, W.; Van der Weken, G.; Verpoort, F.; Vergote, G.; Remon, J. P. *Trends Anal. Chem.* **2002**, *21*, 869.
(14) Lu, Y.; Liu, G. L.; Kim, J.; Mejia, Y. X.; Lee, L. P. *Nano Lett.* **2005**, *5*, 119.
(15) Jiang, J.; Bosnick, K.; Maillard, M.; Brus, L. *J. Phys. Chem. B* **2003**, *107*, 9964.
(16) Hartschuh, A.; Sanchez, E. J.; Xie, X. S.; Novotny, L. *Phys. Rev. Lett.* **2003**, *90*, 095503.
(17) (a) Brown, K. R.; Walter, D. G.; Natan, M. J. *Chem. Mater.* **2000**, *12*, 306. (b) Brown, K. R.; Natan, M. J. *Langmuir* **1998**, *14*, 726. (c) Jana, N. R.; Gearheart, L.; Murphy, C. J. *Langmuir* **2001**, *17*, 6782. (d) Link, S., El-Sayed, M. A. *J. Phys. Chem. B* **1999**, *103*, 4212.
(18) Martin, C. R. *Chem. Mater.* **1996**, *8*, 1739.
(19) Yu, Y. Y.; Chang, S. S.; Lee, C. L.; Wang, C. R. C. *J. Phys. Chem. B* **1997**, *101*, 6661.
(20) Nikoobakht, B.; El-Sayed, M. A. *Chem. Mater.* **2003**, *15*, 1957.
(21) Kim, F.; Song, J. H.; Yang, P. D. *J. Am. Chem. Soc.* **2002**, *124*, 14316.
(22) Nikoobakht, B.; El-Sayed, M. A. *Langmuir* **2001**, *17*, 6368.
(23) Xia, Y.; Yang, P.; Sun, Y.; Wu, Y.; Mayers, B.; Gates, B.; Yin, Y.; Kim, F.; Yan, H., *Adv. Mater.* **2003**, 15, 353 and references therein.
(24) Pérez-Juste, J.; Liz-Marzán, L. M.; Carnie, S.; Chan, D. Y. C.; Mulvaney, P. *Adv. Funct. Mater.* **2004**, *14*, 571.
(25) Jana, N. R.; Gearheart, L.; Murphy, C. J. *J. Phys. Chem. B.* **2001**, *105*, 4065.
(26) Busbee, B. D.; Obare, S. O.; Murphy. C. J. *Adv. Mater.* **2003**, *15*, 414.
(27) Murphy, C. J.; Sau, T. K.; Gole, A. M.; Orendorff, C. J.; Gao, J. X.; Gou, L. F.; Hunyadi, S. E.; Li, T. *J. Phys. Chem. B* **2005**, *109*, 13857.
(28) Nikoobakht, B.; El-Sayed, M. A. *Chem. Mater.* **2003**, *15*, 1957.
(29) Zhang, J. L.; Du, J. M.; Han, B. X.; Liu, Z. M.; Jiang, T.; Zhang, Z. F. *Angew. Chem., Int. Ed.* **2006**, *45*, 1116.
(30) Sun, Y.; Mayers, B.; Xia, Y. *Nano Lett.* **2003**, *3*, 675.
(31) Shankar, S. S.; Rai, A.; Ankamwar, B.; Singh, A.; Ahmad, A.; Sastry, M. *Nat. Mater.* **2004**, *3*, 482.
(32) Millstone, J. E.; Park, S.; Shuford, K. L.; Qin, L. D.; Schatz, G. C.; Mirkin, C. A. *J. Am. Chem. Soc.* **2005**, *127*, 5312.
(33) Li, Z. H.; Liu, Z. M.; Zhang, J. L.; Han, B. X.; Du, J. M.; Gao, Y. N.; Jiang, T. *J. Phys. Chem. B* **2005**, *109*, 14445.
(34) Ah, C. S.; Yun, Y. J.; Park, H. J.; Kim, W. J.; Ha, D. H.; Yun, W. S. *Chem. Mater.* **2005**, *17*, 5558.
(35) Sun, X. P.; Dong, S. J.; Wang, E. K. *Angew. Chem., Int. Ed.* **2004**, *43*, 6360.
(36) Tsuji, M.; Hashimoto, M.; Nishizawa, Y.; Kubokawa, M.; Tsuji, T. *Chem.—Eur. J.* **2005**, *11*, 440.
(37) Zhou, Y.; Wang, C. Y.; Zhu, Y. R.; Chen, Z. Y. *Chem. Mater.* **1999**, *11*, 2310.
(38) Li, C. C.; Cai, W. P.; Cao, B. Q.; Sun, F. Q.; Li, Y.; Kan, C. X.; Zhang. L D. *Adv. Funct. Mater.* **2006**, *16*, 83.
(39) Maillard, M.; Giorgio, S.; Pileni, M. P. *J. Phys. Chem. B.* **2003**, *107*, 2466.
(40) Liang, H. P.; Wan, L. J.; Bai, C. L.; Jiang, L. *J. Phys. Chem. B* **2005**, *109*, 7795.
(41) Halas, N. J. *MRS Bull.* **2005**, *30*, 362.
(42) Oldenburg, S. J.; Averitt, R. D.; Westcott, S. L.; Halas, N. J. *Chem. Phys. Lett.* **1998**, *288*, 243.
(43) Averitt, R. D.; Westcott, S. L.; Halas, N. J. *J. Opt. Soc. Am.* **1999**, *16*, 1824.
(44) Liu, G. L.; Lu, Y.; Kim, J.; Doll, J. C.; Lee, L. P. *Adv. Mater.* **2005**, *17*, 2683.
(45) Sun, Y. G.; Wiley, B.; Li, Z. Y.; Xia, Y. N. *J. Am. Chem. Soc.* **2004**, *126*, 9399.
(46) Sun, Y. G.; Xia, Y. N. *J. Am. Chem. Soc.* **2004**, *126*, 3892.
(47) (a) Sau, T. K.; Murphy, C. J. *J. Am. Chem. Soc.* **2004**, *126*, 8648. (b) Nehl, C. L.; Liao, H. W.; Hafner, J. H. *Nano Lett.* **2006**, *6*, 683.
(48) Chen, S.; Wang, Z. L.; Ballato, J.; Foulger, S. H.; Carroll, D. L. *J. Am. Chem. Soc.* **2003**, *125*, 16186.
(49) Hao, E.; Bailey, R. C.; Schatz, G. C.; Hupp, J. T.; Li, S. Y. *Nano Lett.* **2004**, *4*, 327.
(50) Yamamoto, M.; Kashiwagi, Y.; Sakata, T.; Mori, H.; Nakamoto, M. *Chem. Mater.* **2005**, *17*, 5391.
(51) Kuo, C. H.; Huang, M. H. *Langmuir* **2005**, *21*, 2012.
(52) Liu, M. Z.; Guyot-Sionnest, P. *J. Phys. Chem. B* **2005**, *109*, 22192.
(53) Grabar, K. G.; Freeman, R. G.; Hommer, M. B.; Natan, M. J. *Anal. Chem.* **1995**, *67*, 735.

methods, including transmission electron microscopy, X-ray diffraction techniques, X-ray photoelectron spectroscopy, and the visible−near IR spectrophotometry. The SPR spectral properties of gold nanoparticles vary considerably with the structural changes. The new synthesis approach and the growth mechanism of the 3D thorny nanostructures are useful for creating new nanostructures and functional nanodevices.

Experimental Section

Materials: Hydrochloroauric acid ($HAuCl_4 \cdot 4H_2O$) was from Sigma (USA) and hydroxylamine hydrochloride (NH_2OH) from Aldrich (USA). Silver nitrate ($AgNO_3$), trisodium citrate dihydrate ($Na_3(C_6H_5O_7) \cdot 2H_2O$), concentrated HCl, and HNO_3 were obtained from Beijing Chemical Reagents Company (China). All the chemicals were analytical grade reagents and used without further purification. Distilled water, purified using a nanopure system, was used in the study. The following stock solutions were prepared: 24.3×10^{-3} M $HAuCl_4$; fresh solutions of 38.8×10^{-3} M trisodium citrate, 1.0×10^{-3} M $AgNO_3$, and 40×10^{-3} M NH_2OH were prepared prior to their use. All glassware used was thoroughly cleaned in aqua regia (3 parts HCl, 1 part HNO_3), rinsed with distilled water, and dried in an oven. Unless otherwise noted, the reactions were carried out at room temperature (20−25 °C).

Colloidal Gold Seed Preparation: Colloidal gold seeds were prepared following the method described in ref 53. Fifty milliliters of 1 mM $HAuCl_4$ was brought to a round-bottomed flask under vigorous stirring. Five millilters of 38.8 mM trisodium citrate was rapidly added to the vortex of the boiling solution, resulting in a color change from pale yellow to burgundy. Boiling was prolonged for 10 min. The heating mantle was then removed, while the stirring was continued for an additional 15 min. The resulting solution of colloidal gold particles was characterized by absorption spectroscopy and transmission electron microscopy (TEM, see Figure S1 in the Supporting Information). The colloidal gold nanoparticles obtained were characterized by a maximum absorption at 520 nm and had uniform size (∼14 nm) and shape.

3D Thorny Gold Nanostructure Preparation: The 3D thorny gold nanostructures were prepared via a seed-mediated growth process. Four-tenths of a milliliter of 25×10^{-3} M $HAuCl_4$ and 1.0 mL of 40×10^{-3} M NH_2OH were added to a designated amount of $AgNO_3$ solution. Under vigorous stirring, 0.1 mL of colloidal gold seeds was added rapidly. Within a few minutes after the addition of the colloidal gold solution, the color of the mixture changed from straw yellow to blue to brown, indicating that the thorny gold nanostructures were generated. The resulting solution of colloidal gold was characterized by absorption spectroscopy and TEM techniques.

Sample Characterization: The absorption spectra of the samples were recorded on a Lambda Bio 20 spectrophotometer (Perkin-Elmer Co.). Generally, 3 mL of the colloid particle solution was sampled and measured immediately. The structure and morphology of gold seeds and gold nanostructures were investigated using TEM and X-ray diffraction (XRD) techniques. TEM images were recorded on a JEOL 2010F microscope, employing an accelerating voltage of 200 kV; and high-resolution transmission electron microscopy (HRTEM) analysis was conducted on a Philips CM200 FEG TEM operated at 200 kV and a JEOL 4010 microscope operated at 400 kV. Specimens for TEM measurements were prepared by dispersing the suspension of colloidal gold nanostructures to the holey carbon film on a copper grid. The grid was mounted on the TEM specimen holder for examination after being well-dried in air. XRD patterns of the sample powders were recorded using a Rigaku D/Max-3C, equipped with a rotation anode. A Cu Kα radiation ($\lambda = 0.15418$ nm) and a fixed power source (40 kV and 200 mA) were used. The samples were scanned at a rate of 8° (2θ)/min over a range from 10 to 90°. X-ray photoelectron spectroscopy (XPS) data were obtained with an ESCALab220i-XL electron spectrometer from VG Scientific using 300W Al Kα radiation. The base pressure was about 3×10^{-9} mbar. The binding energies were referenced to the C1s line at 284.6 eV from adventitious carbon.

Results and Discussion

1. Structural Evolution of 3D Thorny Gold Nanostructures. The TEM images of the samples in Figure 1 illustrate an interesting morphological evolution of the gold nanostructures as the concentration of $AgNO_3$ solution increased. For comparison, a reference sample was also prepared under the same experimental conditions but in the absence of $AgNO_3$. The reference is mainly large quasi-spherical gold nanoparticles (Figure 1a),[8,17,42] because spherical nanoparticles have small specific surface area and thus low surface energy.[54]

Obviously, the introduced $AgNO_3$ solution has an important impact on the morphology of the product gold nanoparticles (Figure 1b−i). When a small quantity of $AgNO_3$ was added ($0.025-0.25 \times 10^{-6}$ M), the resulting nanoparticle morphology gradually deviated from the spherical geometry as the amount of Ag^+ ions increased (images b and c of Figure 1), which was also validated from the red-shift of the SRP peak (see below). As the $AgNO_3$ concentration was increased to 0.75×10^{-6} M, gold nanoparticles with short thorns were observed (Figure 1d and the Supporting Information, Figure S2). The further increase in $AgNO_3$ solution to 2.5×10^{-6} M resulted in thorn growth: the gold nanoparticles with long thorns of more than 100 nm were observed (Figure 1f and the Supporting Information, Figure S3). Interestingly, the thorn length no longer increased obviously when the concentration of $AgNO_3$ solution was above 2.5×10^{-6} M (images g−i in Figure 1). The number of the nanothorns on one gold nanoparticle decreased and the central parts of the nanostructures (the body) expanded. All the particles with long thorns like irregular snowflakes have a 3D conformation. Compared with the branched gold nanocrystals obtained in the presence of BSPP, of which structural reconstruction occurred after several days even when they had been kept in a refrigerator,[49] the 3D thorny gold nanoparticles are very stable: no structural change had been observed after they were dispersed in an aqueous solution or on the sample holder of copper grid for TEM at room temperature for 2 months.

The detailed TEM investigations reveal that the crystal structures of the thorns are diverse. According to selected area electron diffraction pattern (SADP) and diffraction contrast analysis, most short thorns are single-domain crystal, which shows even diffraction contrast (see the Supporting Information, Figure S4). No dislocation or stacking fault was observed in the single-crystal short thorns. A dark-field (DF) image was taken in the same area shown in Figure 2a using a {111} reflected beam (Figure 2b). In the DF image, we

(54) Mullin, J. W. *Crystallization*' Butterworths: London, 1961; p 111.

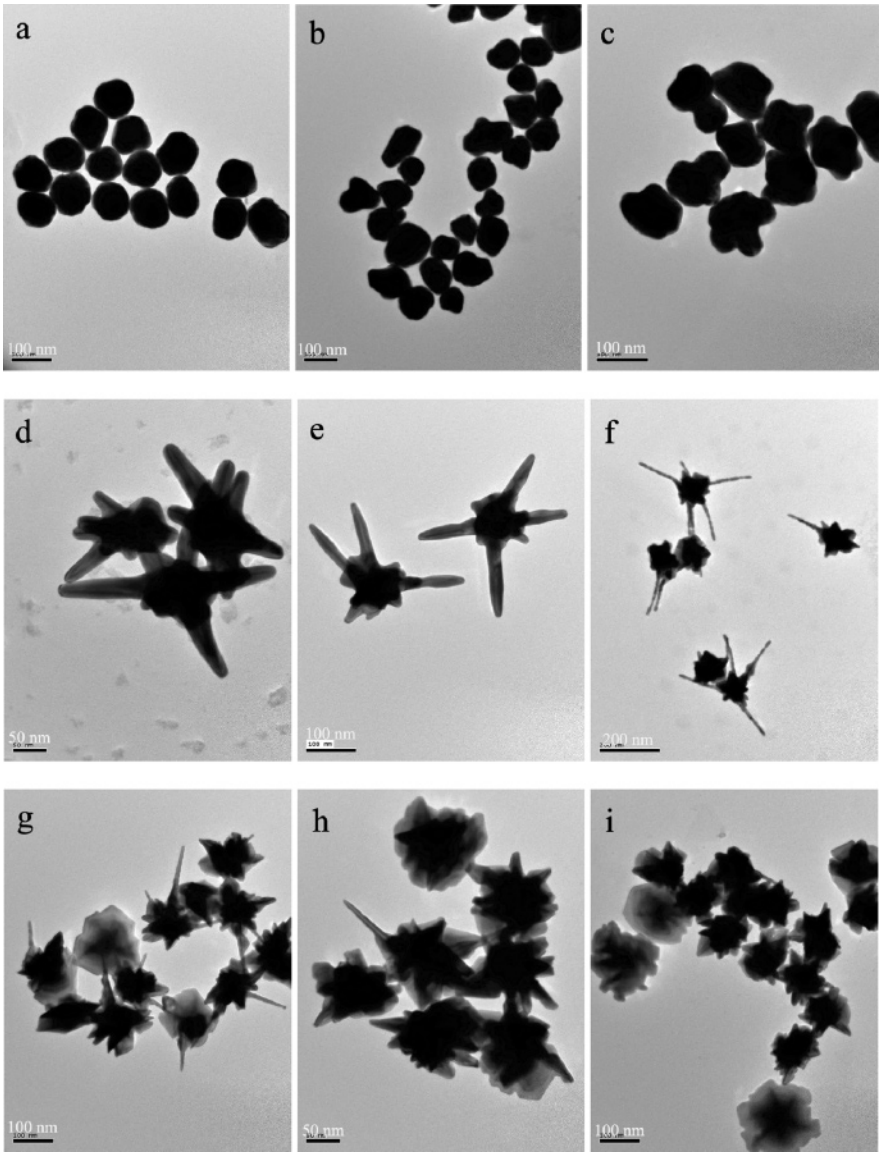

Figure 1. TEM images of gold nanostructures obtained after adding different concentrations of $AgNO_3$: (a) 0, (b) 0.025, (c) 0.25, (d) 0.75, (e) 1.25, (f) 2.5, (g) 7.5, (h) 12.5, and (i) 25×10^{-6} M.

could observe only the crystals whose orientation meets the diffraction conditions, whereas the crystals orienting differently could not be observed.[55] Thus, the short thorn that could be observed entirely in Figure 2b is a single crystal. Short thorns consisted of 2-fold twinned crystals were also found (Figure 2c), although most of the short thorns were single crystals. The electron diffraction pattern in Figure 2d was a typical pattern for twinned crystals of fcc gold structure with indexed zone $[011]_M/[011]_T$. The short thorn in Figure 2c is twinned crystal, and there is a twin plane between the two single crystals. It should be noted that the thorn point downward is 5-fold twinned crystals, and the arrows highlight five crystals (Figure 2a), but the short thorns of 5-fold twinned crystals are rarely observed.

Many 1D gold nanoparticles (nanorods and nanowires) have been found to be single crystals,[19−22,28] though nanorods of 2-fold twinned crystals[23−25,27] and multiple twinned crystals have been reported.[58] In the present study, as shown in Figure 3, most long thorns consisted of 2-fold twinned crystals, which is different from the short thorns. In the bright-field (BF) image, the entire thorn could be seen (Figure 3c), but in the dark-field image (Figure 3d) only a half of the thorn, whose reflected beam was chosen to image, could be observed. The growth axis direction for both short and long thorns of twinned structure was $[2\bar{1}1]$, as indicated in the images. The twin plane between the twinned single crystals α and β is [111]. The crystallography of a twinned nanothorny is illustrated in the Supporting Informaiton, Scheme S1. Such a growth direction of twinned gold nanorods was also reported in the literature.[57]

(55) Wang, Z. L. *J. Phys. Chem. B* **2000**, *104*, 1153.
(56) Tian, M. L.; Wang, J. G.; Kurtz, J.; Mallouk, T. E.; Chan, M. H. W. *Nano Lett.* **2003**, *3*, 919.
(57) Wang, Z. L.; Mohamed, M. B.; Link, S.; El-Sayed, M. A. *Surf. Sci.* **1999**, *440*, L809.
(58) Johnson, C. J.; Dujardin, E.; Davis, S. A.; Murphy, C. J.; Mann, S. *J. Mater. Chem.* **2002**, *12*, 1765.

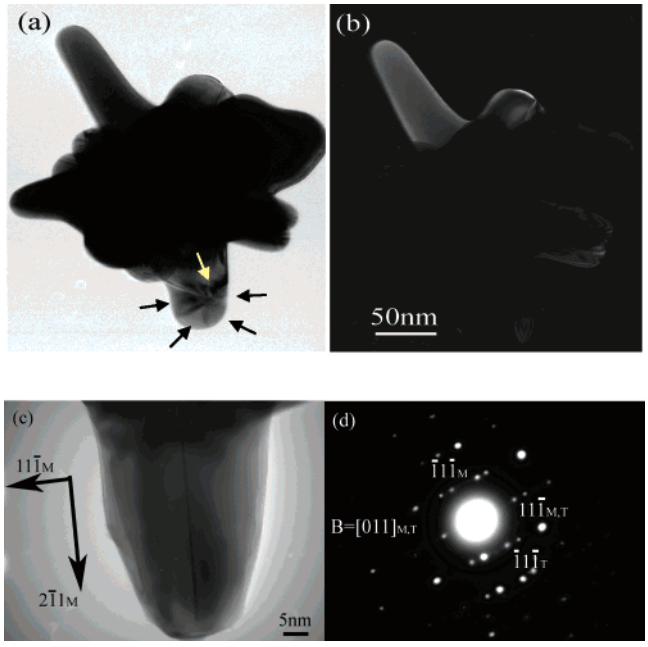

Figure 2. (a) BF image of a single-crystal short thorn of the sample shown in Figure 1d; (b) its central dark-field (CDF) image, taken from $g = [111]$; (c) BF micrograph of a twinned short thorn; and (d) SADP of the twinned short thorn.

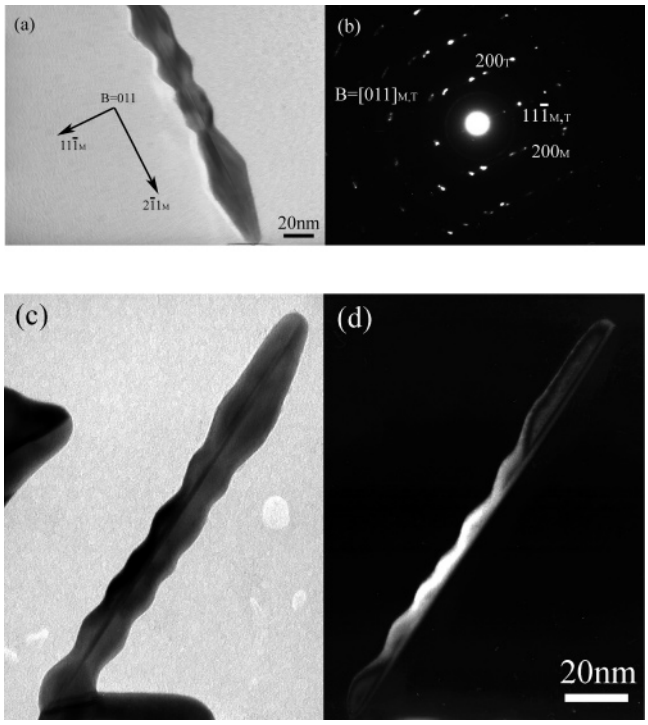

Figure 3. (a) TEM bright-field micrograph of a twinned long thorn; the growth axis direction is $[2\bar{1}1]$; (b) selected area electron diffraction pattern (SADP) of the long thorn in micrograph (a), and the indexed zone $B = [011]_M/[011]_T$; (c) the BF image of a twinned long thorn of the sample shown in Figure 1f; and (d) the CDF image of the twinned long thorn in image (c).

There is a small fraction of the long thorns consisted of 5-fold twin crystal in the thorny gold structures. The growth axis direction was determined (images a and b of Figure 4) as the common close-packed direction $[01\bar{1}]$ of 5-fold twinned nanorods of fcc gold. The interplane spacing of the [111] plane was 0.2355 nm, measured from the high-resolution TEM image (Figure 4b). Such a crystallographic structure of 5-fold twins is consistent with that reported by Johnson and co-workers,[58] but different from that proposed by Gai and Harmer[59] in terms of the growth axis direction and directions of the relative crystal planes. The electron diffraction pattern in Figure 4c was a typical pattern for 5-fold twinned gold structures, and the geometric relationship between the incident electron beam and 5-fold twinned long thorn is illustrated in Scheme S2 of the Supporting Information.

Another unique feature of the long thorns is their corrugated shape. The diameter of an individual thorn varies along the axis of the thorn. The gold nanorods with uniform thickness (flat side surfaces of the rods) were prepared in the presence of the surfactant (CTAB),[19,27,57,59] and the interaction between the surfactant and the side surface (100 planes) play a key role in formation of the smooth surfaces. In the present study, no surfactant or template was introduced, and hence there was no such interaction to confine the shape of the side surfaces of the long thorns, resulting in long thorns with varying thickness. These thorns appear like a string of gold spheres, but they are not a string of spherical crystals attached together. As shown in Figures 2−4, they are twinned crystals elongating along the thorn axis. Therefore, the formation of long thorns could not be explained by the mechanism of the oriented attachment of nanoparticles, in which the primary nanorods attach to each other with the assistance of the micelle template,[60] although it has been widely applied for the construction of 1D semiconductor nanostructures with rough surfaces.[61] The formation of a corrugated shape can result from the physical absorption of AgCl on the surface of growing gold nanothorns (see below), which is analogous to the rough gold nanoparticles shown in images b and c of Figure 1. Such geometry of the long thorns also confirms the confining function of the CTAB surfactants used by other researchers from different point of view.

The XRD patterns of the 3D thorny gold nanoparticles also confirmed that the gold particles are crystalline (see the Supporting Information, Figure S5). The peaks at $2\theta = 38.18$, 44.39, 64.58, 77.54, and 81.76° were assigned as (111), (200), (220), (311), and (222) reflections, respectively, of fcc gold metal (PDF 4-784).

These above results also highlight two possibilities of important consequence: First, it is possible to tailor the morphology of the gold nanostructures by simply varying the amount of the $AgNO_3$ solution. Second, the growth process of the 3D thorny gold nanostructures is different from those reported in literature for the gold nanostructures in the presence of templates or surfactants.[18−47]

(59) Gai, P. L.; Harmer, M. A. *Nano Lett.* **2002**, *2*, 771.
(60) (a) Jana, N. R. *Small* **2005**, *1*, 875.(b) Jana, N. R. *Angew. Chem., Int. Ed.* **2004**, 43, 1536. (c) Leontidis, E.; Kleitou, K.; Kyprianidou, L. T.; Bekiari, V.; Lianos, P. *Langmuir* **2002**, *18*, 3659.
(61) (a) Tang, Z.; Kotov, N. A.; Giersig, M. *Science* **2002**, 297, 237. (b) Lu, W.; Gao, P.; Jian, W. B.; Wang, Z. L.; Fang, J. Y. *J. Am. Chem. Soc.* **2004**, 126, 14816. (c) Cho, K. S.; Talapin, D. V.; Gaschler, W.; Murray, C. B. *J. Am. Chem. Soc.* **2005**, 127, 7140. (d) Pacholski, C.; Kornowski, A.; Weller, H. *Angew. Chem., Int. Ed.* **2002**, 41, 1188. (e) Korgel, B. A.; Fitzmaurice, D. *Adv. Mater.* **1998**, *10*, 661.

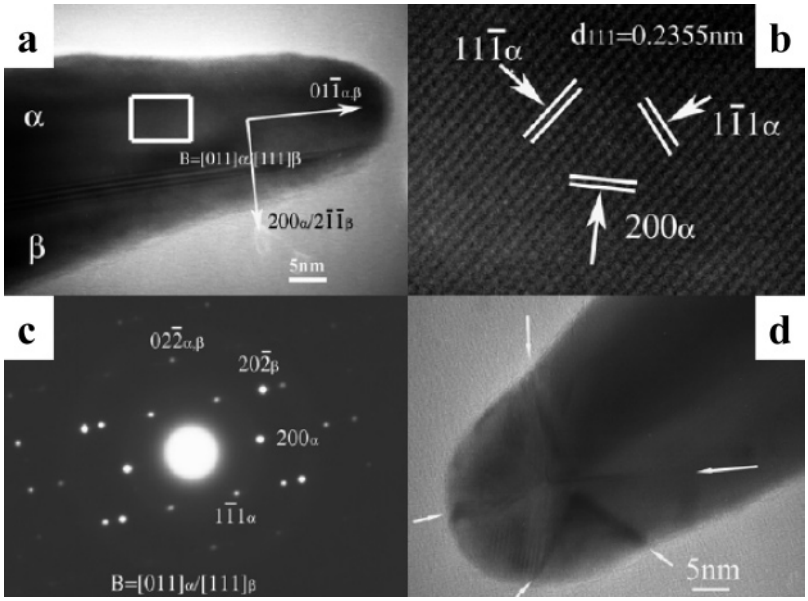

Figure 4. Morphology and crystallography of 5-fold twinned gold nanothorns of the sample shown in Figure 1f: (a) TEM bright-field image of a gold thorn; (b) HRTEM micrograph taken from the rectangle area marked in (a); (c) SADPs corresponding to (a), indexed zone $B = [011]_\alpha/[111]_\beta$; (d) the declining tip of a gold 3D thorn shows the 5-fold twinned structure domains in a long thorn.

The synthesis in the current study should involve the reduction of $HAuCl_4$ by NH_2OH

$$HAuCl_4(aq) \xrightarrow[\text{Au nanoseeds}]{NH_2OH} Au^0(s) + Cl^-(aq) \qquad (1)$$

This reaction is accelerated dramatically on the surface of colloidal gold nanoseeds.[62] In the presence of Ag^+ ions, the Cl^- anions precipitate with the Ag^+ ions

$$Ag^+(aq) + Cl^-(aq) \rightarrow AgCl(s) \qquad (2)$$

When AgCl forms on the surface of the growing gold nanoparticles, the growth process and the morphology of the final Au product are affected inevitably, so that the Au nanoseeds could not isotropically expand to large gold spheres but form the thorny gold nanostructures. The amount of $AgNO_3$ solution, which determines the quantity of AgCl precipitates according to Reaction 2 because the concentration of Cl^- ions is much higher than that of Ag^+ ions in the reaction system, will certainly have a considerable impact on the structure of the gold nanoparticles, as demonstrated in Figure 1. So the physical absorption of AgCl precipitates on the surface of gold nanoseeds decreased their growth rate and led to their unsymmetrical growth, all of which is the source of forming 3D thorny gold nanostructures. Similar knowledge has been used to explain the growth of gold nanostars.[47b] The nucleation of growth anisotropy at multiple sites could be due to a high defect density caused by rapid growth.[47b] The commercial nanoparticle seeds may stimulate rapid growth because of their relatively unprotected surface chemistry compared to the surfactant-stabilized seed nanoparticles that produce gold nanorods.[20]

The presence of silver on the surface of thorny gold nanoparticles was confirmed by the XPS result (see the Supporting Information, Figure S6a). The carbon 1s line position (C 1s in the spectrum) was used as a reference in the XPS measurements. The modified Auger parameter (α) of Ag was calculated to be 724.9 eV. This was in good agreement with that of Ag^+ (724.8 eV), indicating that silver in the gold nanostructures existed in an Ag^+ state. The Au $4f_{7/2}$ binding energy was 83.5 eV (see the Supporting Information, Figure S6b), being close to the value for metallic gold. This meant that $HAuCl_4$ was converted to metallic gold (Reaction 1). It is shown from EDAX data that the AgCl precipitates could be dissolved by the addition of an aqua ammonia solution and then washed off with distilled water (see the Supporting Information, Figure S7), which supports the inference that AgCl precipitates on the surface of gold nanoparticles. However, there was no diffraction peak of AgCl in the XRD pattern. There are two possible reasons for this result. First, the quantity of AgCl is below the detection limit of XRD. Second, AgCl exists in such small structure with poor crystallinity that it cannot give detectable diffraction peak.

The present experimental data show that Ag^+ ions play a key role in the growth of 3D thorny gold nanoparticles in the absence of template or surfactants. Though the growth mechanism of 3D thorny gold nanoparticles could not be fully understood, two control experiments were carried out to further validate that the formation of thorny gold nanoparticles is caused by the introduction of Ag^+ ions.

The first control experiment was the second growth of gold nanoparticles, which was carried out in the aqueous solution of $HAuCl_4$ and NH_2OH using 3D thorny gold nanostructures with long thrones as the seeds. If the $AgNO_3$ solution was not introduced into the reaction system, the 3D thorny gold nanostructures grew to bulky particles (left image in Figure 5). When $AgNO_3$ was also added into the growth solution, the structure of the product gold particles was beyond our anticipation (the right image in Figure 5). New nanothorns formed on the long thorns of the seeds (see inset image and the highlighted circles), so that we observed

(62) Stremsdoerfer, G.; Perrot, H.; Martin, J. R.; Clechet, P. *J. Electrochem. Soc.* **1988**, *135*, 2881.

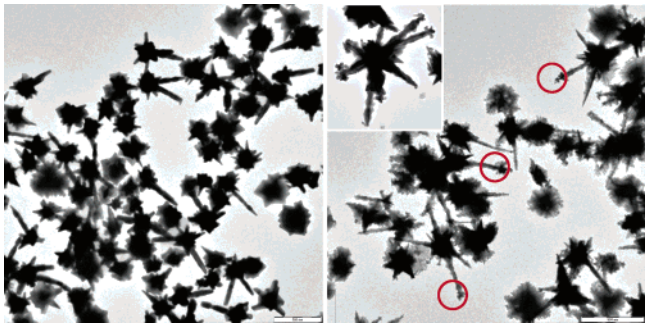

Figure 5. TEM images of gold nanostructures obtained by the second growth in the absence (left) and presence (right) of silver ions. Inset shows a higher-magnification image from gold nanoparticles.

branched thorns similar to the dendritical structures. The second growth of gold nanoparticles led to the formation of branched gold nanostructures, and it is possible to obtain multilevel branched structures by multistep protocol of thorny gold nanoparticles. These results also confirm again that the Ag^+ ions in the synthesis have a decisive impact on the morphology of the final gold nanostructures. The approach of using the 3D thorny gold nanoparticles as seeds can be used to create more complicated gold nanostructures. The controlled growth of multilevel branched nanostructures has great potential for even larger structures and their utilization in nanoscale devices and systems.[6,63−66] A few methods were reported for achieving multilevel branched nanostructures of semiconductor materials.[64−66] For example, Dick et al. reported the controlled stepwise growth of branched semiconductor GaP structures that resemble trees via the vapor−liquid−solid growth mode.[64] A general approach was proposed for fabricating branched semiconductor (II−VI) nanocrystal heterostructures by epitaxially connecting branched and linear junctions within single nanocrystals in homogeneous solutions.[65] To the best of our knowledge, there has been no report on the construction of multilevel branched gold nanostructures. The present study shows that introducing Ag^+ ions into the reaction systems is an effective approach to achieve highly complicated gold nanoparticles and to control the multilevel growth.

To further verify that the silver ions can promote formation of the 3D thorny structure in other systems with $HAuCl_4$ as gold source, the Turkevich method to prepare gold nanospheres was carried out as the second control experiment.[7−9,17] In the present study, a 100 mL mixture solution of 1.0×10^{-3} M $HAuCl_4$ and 1.0×10^{-5} M $AgNO_3$ (Au_{atom}:Ag_{atom} = 100:1) in a rolling boiler was vigorously stirred at 100 °C. Five milliliters of 38.8 mM sodium citrate was then added rapidly to the vortex of the stirred solution, and the heating mantle was immediately removed. The reaction system was stirred until it cooled to room temperature. Because the reduction potential of Ag^+/Ag (0.80 V vs standard hydrogen electrode, SHE) is lower than that of the $AuCl_4^-/Au$ pair (0.99 V vs SHE), AgCl precipitation can be formed in the reaction process. It is known that the citrate on the surface of noble metallic colloids can be displaced by more strongly binding anions, such as halides.[67] So AgCl precipitation can adsorb on the surface of gold nanoparticles and lead to the formation of thorny gold nanoparticles. As illustrated in Figure 6, the product gold nanoparticles had irregular shapes, which considerably deviated from spherical geometry, but were similar to the 3D thorny structure (also see the Supporting Information, Figure S8). The gold nanoparticles obtained in the presence of Ag^+ ions exhibited a broad absorption peak at 730 nm because of the irregular shapes of gold nanoparticles. Similar to the system with NH_2-OH as reducing agent, the AgCl precipitate on the gold surface changes the deposition of gold atoms and leads to the formation of thorny gold nanostructures. The morphological deviation of the resulting gold nanoparticles from the spherical geometry causes the red shift of the extinction peak.

On the basis of all above experimental data, the formation process of the 3D thorny gold nanostructures in the presence of Ag^+ ions can be summarized in Scheme 1.

2. Surface Plasmon Resonance Properties of 3D Thorny Gold Nanoparticles in the Visible−Near-IR Range. The optical properties of gold nanoparticles are dependent on particle shape, size, interparticle interactions, and dielectric constant of the surrounding medium.[7,8] Thus, the structural evolution (illustrated by the TEM images in Figure 1) could result in the variety of the extinction peak of the 3D thorny gold nanostructures. The visible−near IR absorption spectra of the 3D thorny nanoparticles were depicted in Figure 7. The SPR peak of the gold nanoparticles shifted from 606 nm to the red direction (long wavelength) until it reached 916 nm as the concentration of $AgNO_3$ solution increased in the range of $0-2.5 \times 10^{-6}$ M. It is known that the deviations from spherical geometry cause the red-shift.[9] Indeed, one could find a tendency from Figures 1 and Figure 7: the greater the deviation from spherical geometry, the larger the red-shift. This is in good agreement with the results reported in the literature.[9,68] Because the increase in the aspect ratio of gold nanorods can cause considerable red-shift of the SPR,[7−9,18−22] the formation and growth of the thorns on the 3D thorny nanostructures is responsible for further red-shift of the SPR peak (Figure 7a).

However, when the amount of $AgNO_3$ solution was further increased, the red-shift trendency was reversed (Figure 7). The SPR peak of the sample prepared in the presence of 25×10^{-6} M $AgNO_3$ shifted to 856 nm. It was a blue-shift with respect to the peak (at 916 nm) of the 3D thorny gold nanostructure prepared in the presence of 2.5×10^{-6} M $AgNO_3$. As shown in the TEM images of Figure 1, the increase in the concentration of $AgNO_3$ solution above 2.5×10^{-6} M resulted in a decrease in the aspect ratio and the number of thorns and an expansion of the bodies of the 3D thorny gold nanoparticles, leading to a blue shift in their SPR peaks.

(63) Wang, D. L.; Lieber, C. M. *Nat. Mater.* **2003**, *2*, 355.
(64) Dick, K. A.; Deppert, K.; Larsson, M. W.; Martensson, T.; Seifert, W.; Wallenber, L. R.; Samuelson, L. *Nat. Mater.* **2004**, *3*, 380.
(65) Milliron, D. J.; Hughes, S. M.; Cui, Y.; Manna, L.; Li, J. B.; Wang, L. W.; Alivisatos, A. P. *Nature* **2004**, *430*, 190.
(66) Grebinski, J. W.; Hull, K. L.; Zhang, J.; Kosel, T. H.; Kuno, M. *Chem. Mater.*, **2004**, *16*, 5260.
(67) (a) Bell, S. E. J.; Sirimuthu, N. M. S. *J. Phys. Chem. A* **2005**, 109, 7405. (b) Mirkin, C. A. *Inorg. Chem.* **2000**, *39*, 2258.
(68) Wang, H.; Goodrich, G. P.; Tam, F.; Oubre, C.; Nordlander, P.; Halas, N. J. *J. Phys. Chem. B* **2005**, *109*, 11083.

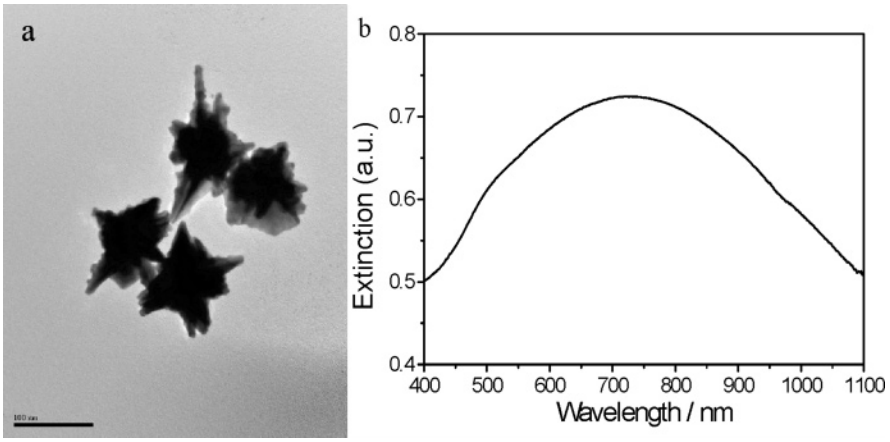

Figure 6. (a) TEM images and (b) vis−near IR extinction spectra of 3D thorny gold nanoparticles obtained by a modified Turkevich method.

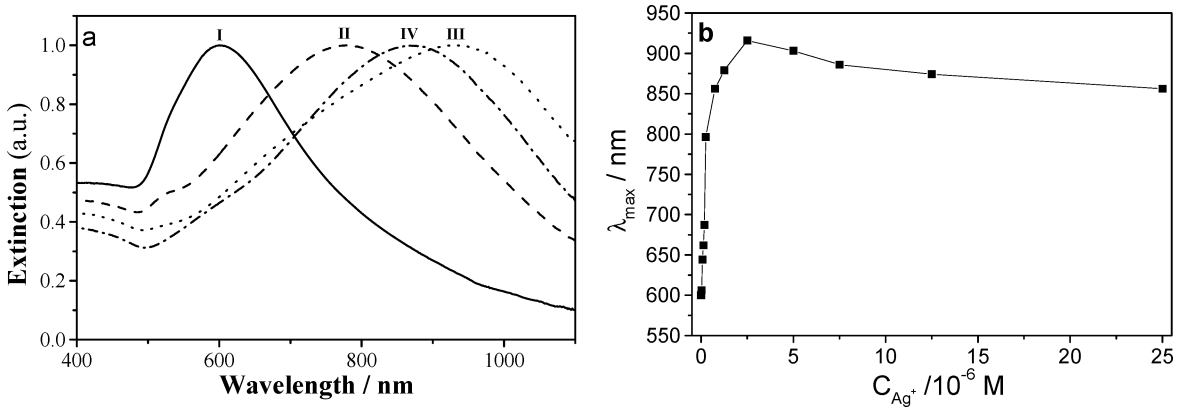

Figure 7. (a) Vis−near IR extinction spectra of aqueous dispersions of gold nanostructures prepared with different concentrations of $AgNO_3$ (I, 0×10^{-6} M; II, 0.25×10^{-6} M; III, 2.5×10^{-6} M; IV, 12.5×10^{-6} M). All spectra are normalized against the intensities of their strongest peaks. (b) The relationship between the maximum absorption wavelength (λ_{max}) of Au nanostructures obtained and the concentration of $AgNO_3$ solution.

Scheme 1. Flowcharts of the Morphological Changes of Au Nanoparticles in the Seed-Mediated Growth

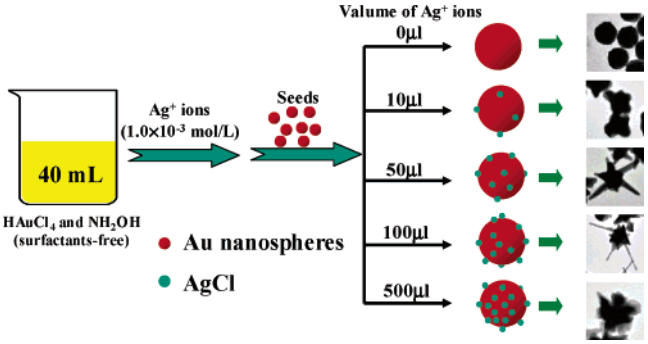

The 3D thorny gold nanoparticles exhibit a high absorption coefficient in the vis−near-IR region (600−1100 nm), which covers the transparent window for tissues. Therefore, these nanostructures have the potential for applications in medicine imaging and biomedical sciences.[4] Besides, there are many junctions in the 3D thorny gold nanoparticles, which are analogous with "SERS hot spots" with greatly enhanced localized electromagnetic field.[7,15] And the tip of the thorns is like that of the gold nanorods reported, which may act as "lightning rod effect" for SERS.[7] Therefore, the 3D thorny gold nanostructures are hoped to have significant potential for SERS probes.

Conclusions

In this study, a simple synthesis approach for the 3D thorny gold nanostructures is reported. It is found that the morphology of the 3D thorny gold nanoparticles and the structure of the gold nanothorns should be controlled by the amount of Ag^+ ions introduced into the reaction systems of $HAuCl_4$ and NH_2OH in the absence of templates and surfactants. The formation and structural changes of the 3D thorny gold nanoparticles can be explained by the deposition of AgCl precipitates on the surface of gold nanoseeds. Moreover, complicated dandrimer-like structures can be achieved by the second growth (using the thorny nanoparticles as seeds in the presence of Ag^+ ions but in the absence of surfactants and template). The colloidal solutions of the 3D thorny gold nanoparticles exhibit a broad absorption peak at 600−1100 nm in the visible and near-infrared range. This synthesis approach offers great opportunities for the design of novel materials with improved spectral and structural properties. The 3D thorny nanostructures provide new structural diversity for the applications in chemical sensing, medicine, and life science and can be used as building blocks of nanoscale electronic and optical devices.

Note Added in Review

After this work was submitted, the authors noticed two very recent publications on the effect of Ag^+ on the

growth of noble metallic nanoparticles: (a) Grzelczak, M.; Pérez-Juste, J.; Rodríguez-González, B.; Liz-Marzán, L. M. Influence of Silver Ions on the Growth Mode of Platinum on Gold Nanorods. *J. Mater. Chem.* **2006**, *16*, 3946−3951. (b) Seo, D.; Park, J. C.; Song, H. Polyhedral Gold Nanocrystals with O_h Symmetry: From Octahedra to Cubes. *J. Am. Chem. Soc.* **2006**, *128*, 14863−14870.

Liz-Marzán's paper focused on the synthesis of Au@Pt nanorods, in which gold nanorods were used as seeds; the group used a mild reducing agent (ascorbic acid) to react with K_2PtCl_4 in the presence of the cationic surfactant CTAB. It is proved that the deposition mode of platinum on gold nanorods can be effectively tuned by removing or keeping Ag^+ ions used during gold nanorod formation (see a). According to Song's paper, when a modified polyol process was used to prepare shaped gold nanoparticles in the presence of PVP, the rapid reduction of gold precursors in refluxing 1,5-pentanediol has successfully provided a series of gold nanocrystals in the shape of octahedra, truncated octahedra, cuboctahedra, cubes, and higher polygons by incremental changes of silver nitrate concentration (see b). Both papers indicate that introducing Ag^+ ions can alter the shape of the resulting nanoparticles, and their morphologies can, to a certain extent, be controlled by the amount of Ag^+ ions. Readers are encouraged to read these publications.

Acknowledgment. We gratefully acknowledge financial support from the 973 Program (2003CB415006), NSFC (20537010 and 20520120221), and CAS.

Supporting Information Available: Two control experiments as noted in text. TEM images, scheme, XRD, XPS, and vis−NIR data. This material is available free of charge via the Internet at http://pubs.acs.org.

CM062046I